Study on efficiency improvement of agricultural irrigation pumping system using brushless DC motor in electrical automation technology

Abstract: Electrical automation technology is applied to the construction of agricultural irrigation pump system to form a complete new agricultural irrigation system, which provides strong support and guarantee for modern agricultural development and scientific water supply. The article combines the Internet of Things technology and electrical automation technology to establish the framework of agricultural irrigation system, and combines the brushless DC motor to realize the integrated irrigation pump integrated intelligent valve control. Combined with the evapotranspiration of crops in actual growth, the crop evapotranspiration prediction model is constructed, and the effective utilization coefficient of agricultural irrigation water is measured using the first and last measurement analysis method. For the intelligent control of agricultural irrigation pumps, this paper takes STM32 microcontroller as the basis, constructs the brushless DC motor control strategy, and designs the corresponding inverter drive protection circuit, and then carries out the effectiveness verification and analysis. The results show that the phase current fluctuation range is stabilized between 12.01A~17.75A under the brushless DC motor control strategy based on STM32. The combined net irrigation water volume of pepper and tobacco after the introduction of the agricultural irrigation pump system was lower than the actual net irrigation water volume by 1481.86 and 211.88 m^3/hm^2, respectively, and the error between the predicted and actual irrigation volume of this system was no more than 3.57% at the maximum. Therefore, the introduction of brushless DC motors into agricultural irrigation systems can maximize the use of water resources for agricultural irrigation.

Keywords: Brushless DC motor, agricultural irrigation system, effective utilization factor of irrigation water, STM32 microcontroller.

1. Introduction

China has a large volume of water used for agricultural irrigation, and the problems of irrigation inefficiency and water wastage are widespread. At present, the irrigation water utilization rate and food productivity per square meter of water in China are much lower than those in developed countries [1-4]. Therefore, it is of great practical significance and far-reaching historical significance to transform traditional irrigated agriculture by adopting modern water-saving irrigation technology to realize "fine irrigation" in the right amount and at the right time [5-7]. The rational use of brushless DC motors in the irrigation system, not only can improve resource utilization, alleviate the contradiction of water resources are increasingly tense, but also increase crop yield, reduce the cost of agricultural products [8-11].

Brushless DC water pump is one of the masterpieces of modern science and technology, which is characterized by its high efficiency, reliability and intelligence, and has been importantly used in agricultural irrigation pumping system. Its working principle utilizes the "electromagnetic induction" principle of electric motor, which is composed of rotor and stator [12-15]. In a brushless DC water pump, the motor is a stator, the rotor is a rotor, the stator is connected to the motor casing through the windings, and at one end of the casing there is a hole for the power supply, through which the motor can be controlled to start and stop [16-19]. Brushless DC water pump is added to the motor in a "commutator", called commutator, commutator outside a "magnetic pole", as the motor rotor rotation will produce a magnetic field, and there is a magnetic pole on the side of the magnetic field by the action of the current will be generated, when the current When there is a current, it will produce induced voltage in the stator winding [20-23]. The induced voltage generates an induced current inside the motor, so that the speed of the motor can be changed by controlling the size of the induced current [24-25].

With the continuous development of big data, cloud computing, electrical automation and other technologies as well as the continuous improvement of

hardware technology, the future agricultural irrigation pump system will play a more important role in efficient water conservation. In this paper, the agricultural irrigation pump system is constructed from the design of the agricultural irrigation pump system, combining the Internet of Things technology and electrical automation technology. Then combined with the crop transpiration to establish a smart irrigation digital model, and through the first and last measurement analysis method to measure the effective utilization coefficient of crop irrigation water. In the integrated intelligent valve control of agricultural irrigation pump system, brushless DC motor control strategy was constructed by using STM32 microcontroller, and inverter drive protection circuit was designed. Finally, data analysis was carried out from the perspectives of control effect, effective utilization coefficient of irrigation water and effectiveness of irrigation pump system to verify the feasibility of the application of brushless DC motor in agricultural irrigation pump system.

2. Agricultural irrigation pumping system architecture design

In recent years, countries around the world have been vigorously promoting and applying smart water-saving irrigation equipment to alleviate the agricultural water crisis and promote the modernization of the agricultural industry. China has also been increasing the development of advanced water-saving irrigation technology, especially the promotion and popularization of smart water-saving irrigation, and actively learning from the energy-saving irrigation experience and technology of advanced countries, so as to further improve the effect of water-saving irrigation in Chinese agriculture. The advanced irrigation equipment and facilities are expensive and complicated to operate, making it impossible for them to be widely used in China. In view of this situation, it is necessary to increase the research efforts on the application of electrical automation technology in agricultural water-saving irrigation, give full play to the advantages and value of these technologies, and realize scientific and intelligent water-saving irrigation, so as to effectively alleviate the status quo of China's agricultural water tension.

2.1 Design of agricultural irrigation pumping systems

2.1.1 Overall system architecture

In order to realize real-time monitoring, data acquisition, automated irrigation control and optimal allocation of water resources in modern agricultural irrigation, this paper designs an agricultural irrigation pump system based on the Internet of Things and brushless DC motors, whose specific structure is shown in Fig. 1, which is mainly composed of two modules: automated irrigation and information management [26]. The automated irrigation module integrates humidity, nitrogen fertilizer sensors, flow meters, etc., and relies on STM32 microcontroller and HMI to realize precise irrigation regulation. The information management module is connected through the cloud platform to ensure remote control and information synchronization. Adopting Siemens STM32 series microcontroller, its modularized design efficiently handles data, and with SMART IE monitoring equipment, it intuitively monitors the environmental parameters and controls the irrigation efficiency of the brushless DC motor. The system is set to collect data every 2 minutes, intelligently determine the soil water holding rate, and control the brushless DC motor to start or stop the water pump and solenoid valve at the right time to ensure accurate and efficient agricultural irrigation. The information management module is an important part of the agricultural irrigation system, connected through the cloud platform to ensure remote control and information synchronization. The module is responsible for data storage, analysis and management, and provides decision support.

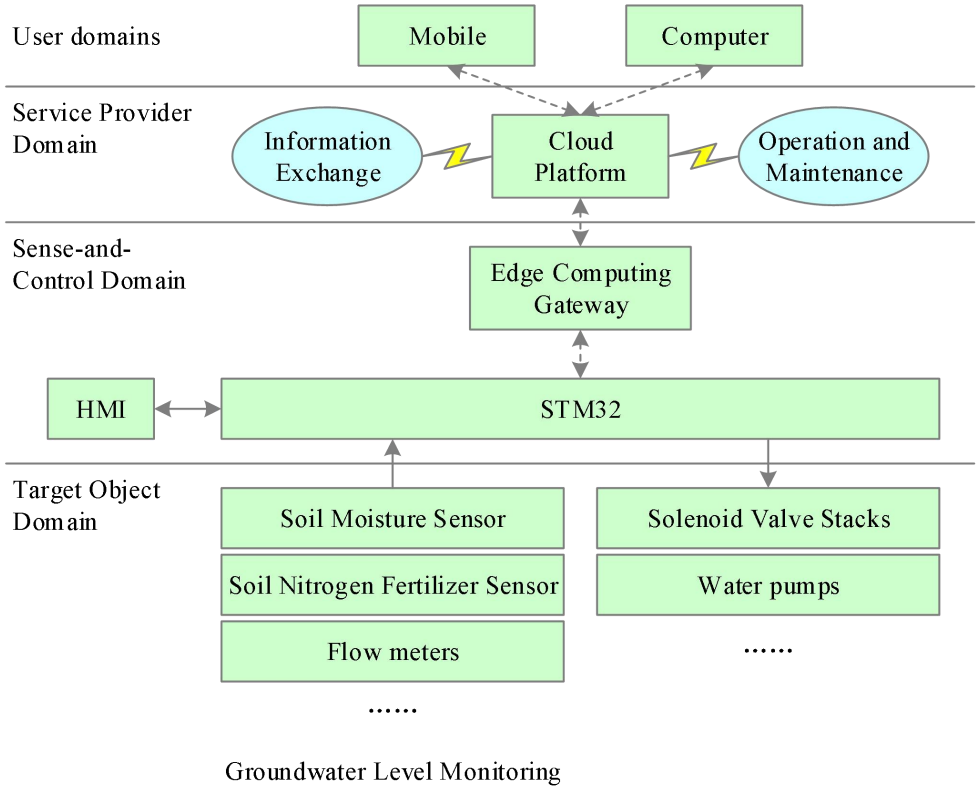

Figure 1 Agricultural irrigation pump system architecture

2.1.2 Intelligent valve control

Integrated intelligent valve regulation is an important node of the agricultural irrigation pump system, whose main function is to receive commands from the irrigation optimization program of the host computer, and control the brushless DC motor to realize the valve opening regulation of irrigation, and then realize the flow regulation. Traditional electric valve control, generally take the wired power supply. In order to reduce cable laying work, reduce cable costs, improve the flexibility of the valve layout, this paper integrated intelligent valve using photovoltaic battery power supply. Integrated intelligent valve control system block diagram shown in Figure 2, mainly consists of photovoltaic modules, batteries, realize the MPPT function of battery charging DC/DC circuit, trip switch detection, water level detection for flow measurement, brushless DC motor control circuit and other components.

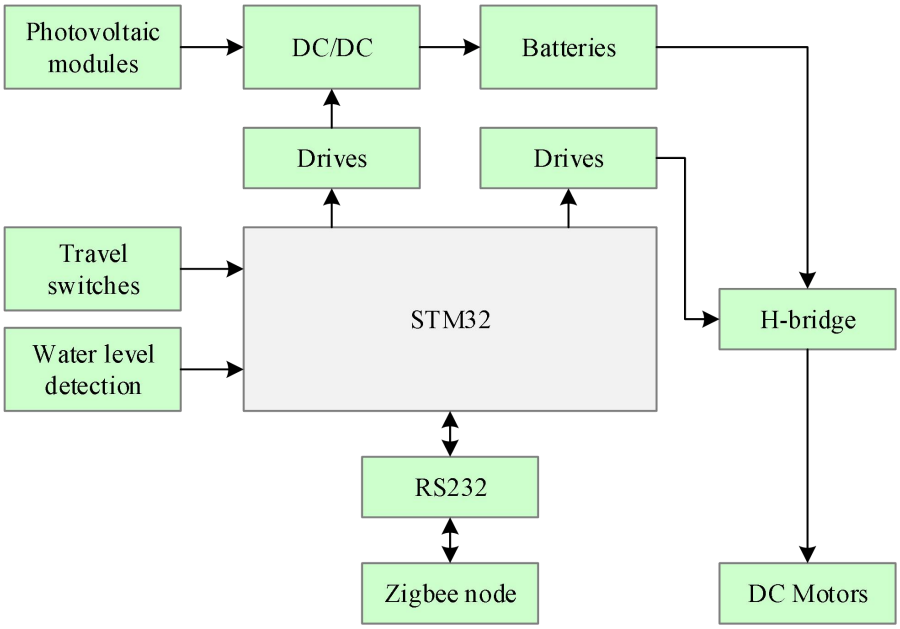

Figure 2 Integrated intelligent valve control system

The most basic function of an integrated valve is flow control, which is realized by controlling the valve opening, and valve control requires accurate position or speed detection. For brushless DC motor to achieve its high precision position control, motor speed and position regulation are usually introduced into the closed-loop control, and speed feedback as an important parameter to realize the motor closed-loop control, has an indispensable role. At present, it is usually adopted to utilize Hall sensors, photoelectric encoders, speed generators and other sensors to realize the measurement and feedback of rotational speed. In this paper, a brushless DC motor control strategy is designed using STM32 microcontroller for speed estimation. While the position of the valve is the integral of the motor speed and is related to the mechanical transmission ratio, this paper utilizes the fully closed and fully open signals of the valve for calibration. And it realizes the measurement and adjustment of arbitrary valve opening without installing a speed sensor, which reduces the overall cost and improves the reliability of the system.

2.2 Modeling of agricultural irrigation systems

2.2.1 Modeling of crop transpiration

To build a more modern agricultural irrigation system, it is necessary to combine the evapotranspiration of crops in the actual growth, accordingly to implement

irrigation management. So the crop root system water absorption layer belongs to the irrigation target arrival layer. The transpiration digital model is established as follows:

$$ET_0 = \frac{0.408\Delta\left(R_n - G\right) + \gamma \times \frac{900}{(273+T)} \times \mu\left(e_s - e_a\right)}{\Delta + \gamma(1 + 0.34\mu)} \tag{1}$$

ET_0 is the evaporative transpiration of crops, Δ is the slope relationship between temperature change and saturated water vapor pressure, R_n is the radiation on the surface of crops, G is the soil heat flux, Y is the wet and dry table constants, T is the average air temperature at the selected reference altitude, μ is the average wind speed at the selected reference altitude, e_s is the saturated water vapor pressure, and e_a is the actual water vapor pressure [27].

In the above formulas, soil moisture belongs to the important indexes, and the difference values and changes of soil moisture at different times are selected, and with the help of process control, multilingual variables are set, while the control theory formulas of intelligent irrigation system for agricultural production are constructed as follows:

$$K_e = \frac{n_1}{\left|e_{\max}\right|} \tag{2}$$

$$K_{ec} = \frac{n_2}{\left|e_{c\max}\right|} \tag{3}$$

$$K_u = \frac{\left|\mu_{\max}\right|}{m} \tag{4}$$

Where K_e is the quantization factor of the error, K_{ec} is the quantization factor of the rate of change of the error, and K_u is the scaling factor of the fuzzy control. n_1 is the fuzzy theoretical domain extremum of error, n_2 is the fuzzy theoretical domain extremum of error rate of change, m is the fuzzy theoretical domain extremum of signal output variable, $e_{\max}$ is the basic theoretical domain extremum of

error, $e_{c\max}$ is the basic theoretical domain extremum of error rate of change, $\mu_{\max}$ is the basic theoretical domain extremum of signal output variable.

2.2.2 Effective utilization factor of irrigation water

In this paper, the first and last measurement analysis method is used for the measurement of effective utilization coefficient of irrigation water, and the calculation formula of net irrigation per mu for a typical field is:

$$W_{\text{Net}} = 0.667 \frac{\gamma}{\gamma_{\text{Water}}} H\left(\theta_{g2} - \theta_{g1}\right) \tag{5}$$

Where W_{Net} is the average net irrigation water per mu of a typical field for a particular irrigation, H is the depth of the wetted layer of the soil plan for a typical field, γ is the dry volumetric mass of soil within the H soil layer of a typical field, γ_{Water} is the volumetric mass of water, θ_{gl} is the water content of soil mass within the H soil layer of a typical field prior to irrigation, and θ_{g2} is the water content of soil mass within the soil layer of a typical field H after irrigation [28].

The gross irrigation water use of a typical field was calculated as:

$$W_{\text{Hair}} = QT \tag{6}$$

Where W_{Hair} is the gross irrigation water use of a typical field for a particular irrigation, Q is the water flow rate of a particular irrigation measured at the diversion wellhead of a typical field, and T is the duration of a particular irrigation in a typical field.

The effective utilization coefficient of irrigation water for a typical field is calculated as:

$$\eta = \frac{W_{\text{Net}}}{W_{\text{Hair}}} \tag{7}$$

Where η is the effective utilization coefficient of irrigation water for a typical field, W_{Net} is the net irrigation water volume for a type of field, and W_{Hair} is the

gross irrigation water volume for a typical field.

According to the active depth distribution of the root system during the development of crops, the wet layer was selected as 1.5 m in the calculation of the effective utilization coefficient of irrigation water, and soil samples were taken in three layers at each measurement point arranged in a typical field. Dry soil samples were taken within 1 day before irrigation, and wet soil samples were taken about 48 h after irrigation, with the number of samples taken depending on the farming habits of the farmers and the distribution of effective rainfall. The soil moisture content of each soil sample was determined by drying and weighing method, and the average value of the soil moisture content of each of the above three layers was taken as the soil moisture content in the planned wet layer, and the irrigation water flow rate of each typical field was measured using ultrasonic pipeline tachometer, and the duration of the irrigation was checked by on-site measurements and inquiries to the head of the household. The effective utilization coefficient of irrigation water for different typical fields was calculated by substituting the measured data into the previous equation.

3. Agricultural irrigation pump system control strategy

In modern society, the Internet of Things and electrical automation technology is becoming more and more mature, and is widely used in various fields, in which the CPU, sensors and other hardware equipment and supporting software control programs are increasingly optimized. The healthy growth of crops needs to be supported by advanced irrigation technology and equipment, over-irrigation will cause crops to breed a large number of bacteria, and under-irrigation will lead to a decline in crop yields. In order to strongly enhance the level of agricultural automation, modernization, rational irrigation, the need to introduce the Internet of Things and electrical automation technology, to actively build agricultural irrigation systems, in order to achieve the scientific use of agricultural irrigation water.

3.1 Brushless DC motor with STM32

3.1.1 Brushless DC motor modeling

This paper takes a two-pole three-phase brushless DC motor as an example, the

stator winding of the motor is Y-type connection, the drive circuit is a three-phase full-bridge circuit, and the operation mode is two-two conduction (three-phase six states). The simplified analysis process assumes the following.

(1) Neglect motor core saturation, no eddy current hysteresis loss, and no armature reaction.

(2) Three-phase winding parameters are the same, Hall sensors are placed 120° apart.

(3) Power tubes and continuity diodes are ideal components.

Under the above assumptions hold true the brushless DC motor (BLDC) voltage balance equation is obtained expressed as:

$$\begin{bmatrix} U_a \\ U_b \\ U_c \end{bmatrix} = \begin{bmatrix} R_a & 0 & 0 \\ 0 & R_b & 0 \\ 0 & 0 & R_c \end{bmatrix} \begin{bmatrix} i_a \\ i_b \\ i_c \end{bmatrix} + \frac{d}{dt} \begin{bmatrix} L_a & L_{ab} & L_{ac} \\ L_{ha} & L_b & L_{bc} \\ L_{ca} & L_{cb} & L_c \end{bmatrix} \begin{bmatrix} i_a \\ i_b \\ i_c \end{bmatrix} + \begin{bmatrix} e_a \\ e_b \\ e_c \end{bmatrix} \tag{8}$$

Where U_a, U_b, U_c for the stator winding phase voltage, R_a, R_b, R_c for the phase resistance, i_a, i_b, i_c for the phase current, L_a, L_b, L_c for the winding self-inductance, L_{ab}, L_{ac}, L_{ha}, L_{bc}, L_{ca}, L_c for the mutual inductance between the windings.

Among them:

$$\begin{cases} R_a = R_b = R_c = R \\ L_{ab} = L_{ac} = L_{ta} = L_{bc} = L_{ca} = L_{cb} = M \end{cases} \tag{9}$$

Since the three-phase currents satisfy $i_a + i_b + i_c = 0$. Thus equation (8) can be rewritten as:

$$\begin{bmatrix} U_a \\ U_b \\ U_c \end{bmatrix} = \begin{bmatrix} R_a & 0 & 0 \\ 0 & R & 0 \\ 0 & 0 & R \end{bmatrix} \begin{bmatrix} i_a \\ i_b \\ i_c \end{bmatrix} + \frac{d}{dt} \begin{bmatrix} L-M & 0 & 0 \\ 0 & L-M & 0 \\ 0 & 0 & L-M \end{bmatrix} \begin{bmatrix} i_a \\ i_b \\ i_c \end{bmatrix} + \begin{bmatrix} e_a \\ e_b \\ e_c \end{bmatrix} \tag{10}$$

The power and torque of the brushless DC motor are analyzed and derived based

on energy transfer. The assumptions above are based on the premise that, neglecting the mechanical and stray losses of the rotor, there is no loss between the electromagnetic power and kinetic energy, i.e., all the electromagnetic power is converted into kinetic energy [29]. Where T_e is the electromagnetic torque and Ω is the mechanical angular velocity of the motor. i.e:

$$P_e = e_a i_a + e_b i_b + e_c i_c = T_e \Omega \tag{11}$$

The equation of motion of the motor is:

$$T_e - T_L = J \frac{d\Omega}{dt} + B_V \Omega \tag{12}$$

where T_L is the torque load, J is the rotor moment of inertia, and B_V is the coefficient of viscous friction.

3.1.2 STM32 Microcontroller

The STM32 family consists of ARM Cortex®-M0, M³, M4, and M7 core types that provide high performance, low cost, and low power consumption for embedded technology applications. Commercial products specifically include STM32F0 models, STM32F1 models, STM32F3 models, ultra-low power products including STM32L0 models, STM32L1 models, STM32L4 models, STM32L4+ models, and high power products including STM32F2 models, STM32F4 models, and STM32F7 models, STM32H7 models.

The STM32 family features fast startup that wakes the microcontroller from stop mode in less than 6 μs. The Energy Lite™ ultra-low power technology platform maximizes energy efficiency in both active and sleep modes. In addition, the platform's embedded Flash memory utilizes ST's proprietary low-power Flash technology. The platform also integrates Direct Memory Access (DMA) support, which reduces the speed of the flash memory and CPU while the application is running, thus supporting normal operation of peripheral devices.

In order to realize effective control of the brushless DC motor in the agricultural irrigation pump system, the main controller chip selected in this paper is a 32-bit microcontroller based on the ARM Cortex-M7 core, STM32F4072ZGT6, which is a

high-performance 32-bit microcontroller chip belonging to STMicroelectronics' STM32F4 series, adopting Arm Cortex-M7 core with powerful computing and processing capabilities, widely used in intelligent control, industrial automation, embedded systems and other fields. This system needs to use STM32's timer to realize the drive motor servo system, so it needs a high rate timer to control the PWM generation, so it is fully satisfied by using STM32F4072ZGT6.

3.2 Brushless DC motor control system

3.2.1 Motor Control Strategy Design

The brushless DC motor control strategy based on STM32 microcontroller is shown in Fig. 3. In the agricultural irrigation system, the general steps for controlling the brushless DC motor to turn on the irrigation pump are as follows:

The controller determines the current position of the motor rotor through the signal feedback from the Hall sensor, which controls the on-off of the switching tubes in the three-phase bridge drive circuit. The continuous change of the switching tube on and off makes the motor form a changing magnetic field, driving the rotor rotation. At the same time, the controller also adjusts the motor speed by adjusting the PWM duty cycle, so that the motor rotates at a specific speed. When the system is in operation, six PWM signals are sent from the STM32F407, which are transmitted through the isolation device to the driver circuit composed of IR2110S. According to the PWM signals, the driver circuit controls the on-off of the 6 switching tubes to form a rotating magnetic field to rotate the motor. The feedback signal from the Hall sensor is transmitted to the STM32 through the isolation chip for it to determine the rotor position and thus implement the commutation operation [30]. In addition, the STM32 can calculate the rotational speed through the Hall signals, and then compare the actual rotational speed with the set rotational speed, and then adjust the duty cycle of the PWM through the PID control algorithm, i.e., adjust the rotational speed, so that the motor will rotate according to the set rotational speed in the end. The keypad circuit can control the motor's start, stop, acceleration, deceleration and forward/reverse rotation by pressing keys. The upper computer can also control the

start and stop of the motor, as well as give the speed value and PID value, and at the same time display the actual speed change curve, which is convenient for the PID parameter adjustment.

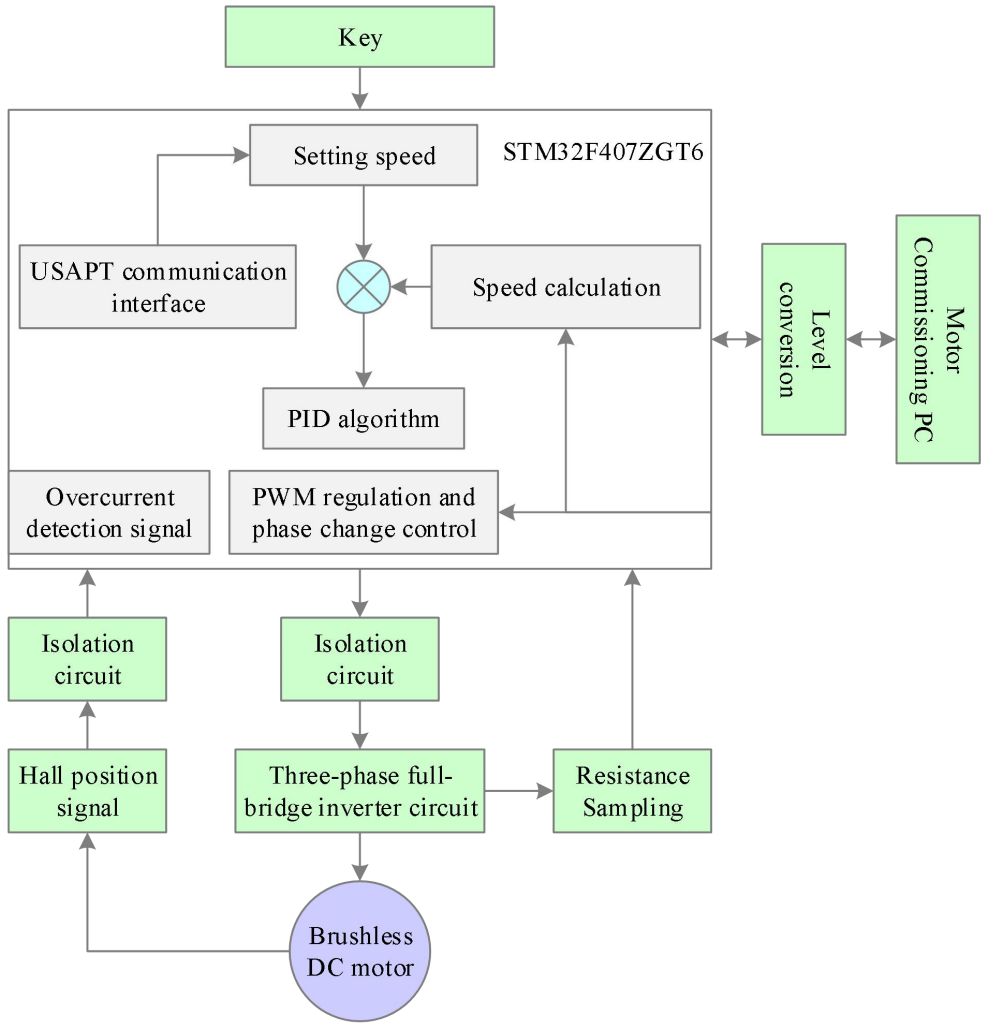

Figure 3 No brush and direct treatment strategy

In the actual control of agricultural irrigation pump system, the motor should run stably according to the required speed, and the speed adjustment process should be rapid and smooth, which can not be realized in the open-loop system, so it is necessary to take the motion control system commonly used PID control algorithms for closed-loop speed control.PID control is the proportional, integral, differential control of the deviation, which is the error control. The proportional part (P) is used to reduce the deviation between the actual speed and the target speed, the larger P is, the faster the deviation is reduced, but in order to avoid system oscillation, the value of P

cannot be too large. The integral part (I) is the accumulation of the speed deviation until the deviation is 0. The integral result is constant and the control action is stable, so the integral part can eliminate the static difference of the system. The differential part (D) can be over-adjusted according to the trend of the deviation to reduce the oscillation of the system and stabilize the system.

3.2.2 Inverter Driver Protection Circuitry

(1) Inverter Driving Circuit

In this study, STM32 is used to drive the power switching tube to control the operation of the brushless DC motor, and the control signals are input through the HIN and LIN ports of the STM32, and then output from the HO and LO ports on the chip after processing. In order to reduce the ringing phenomenon and smoothing the gate charging current, this study connects a resistor to the signal output of the chip, which has the advantage of preventing the ringing phenomenon, the output port of the chip STM32 will carry some stray inductance, which may form an LC oscillation with the gate capacitor when the voltage changes suddenly, and when the MOS tube is connected in series with a resistor, it increases the damping and reduces the oscillation. Reduce the gate charging peak current, when the gate voltage is pulled up, the first gate capacitor charging, in order to prevent the charging current is too large, series resistance can increase the charging time, reduce the gate charging peak current.

(2) Over-current protection circuit

In the whole brushless DC motor control system, MOS tube is the most critical and fragile link, often due to excessive current or high temperature in actual operation leads to MOS tube burnt. Therefore, direct measures are taken in hardware to avoid MOS tube burning. Bus current through the resistance sampling and two ceramic capacitors to remove high-frequency harmonics, DCBUSC signal, through the comparator LM 358 and the hardware circuit to set the voltage compared to the results of the comparison is input to the monostable trigger by the 555 chip to build a monostable circuit on the transient low-level response fast, and the duration of the response time is stable, and can be effectively detected in each overcurrent state. The overcurrent signal is input to the tri-state gate enable terminal of the STM32 chip of

the bus transceiver. When an overcurrent occurs in the hardware circuit, the tri-state gate enable terminal transmits the MOS tube switching signal sent from the prohibited microcontroller to the STM32 chip. Therefore, the MOS tube is turned off completely, pinching off the bus current and protecting the hardware circuit.

4. Application validation of agricultural irrigation systems

China has a long-standing problem of oversupply of water for agricultural irrigation, and according to surveys, the amount of water consumed in agricultural irrigation accounts for 3/4 of China's total annual water consumption. In contrast, in some countries with more developed intelligent technology, the effective utilization coefficient of agricultural irrigation water resources reaches more than 0.7, indicating that intelligent technology is a good channel to improve the utilization of agricultural irrigation water resources. In order to meet the demand for agricultural irrigation water resources in various regions of China, and to improve the rationality and efficiency of water resources utilization, this paper combines the Internet of Things and electrical automation technology to transform the traditional agricultural irrigation mode into a smart agricultural irrigation system, which in turn provides a reference for improving the actual utilization efficiency of agricultural irrigation water resources in China.

4.1 Control effect of brushless DC motor

4.1.1 Simulation Modeling

Under the Simulink environment of MATLAB, using the rich module library provided by Sim Power System Toolbox, the method of establishing the simulation model of BLDC control system is proposed on the basis of analyzing the mathematical model of BLDC.The BLDC modeling and simulation system adopts a double closed-loop control scheme, in which the rotational speed loop is composed of a PID regulator, and the current loop is composed of a current hysteresis loop regulator. According to the idea of modular modeling, the agricultural irrigation pump control system established in the previous section is divided into various functionally independent sub-modules. These mainly include the BLDCM body module, speed

control module, reference current module, current hysteresis loop control module, torque calculation module and voltage inverter module. Combining these functional modules with the S-function, the simulation model of the BLDC control system is built in MATLAB/Simulink, and the control algorithm of the double closed-loop is realized.

In the simulation, the parameters of BLDC motor are set as stator phase winding resistance of 2Ω, stator phase winding self-inductance of 0.03L, rotational moment of inertia of 0.004kg-m², damping coefficient of 0.0003N-m-s/rad, rated rotational speed of 800r/min, pole-pair number is 1, and 220V DC power supply is supplied. The three parameters of the discrete PID controller K_p, K_i, K_d are 5, 0.01 and 0.001 respectively, the saturation limit module amplitude is limited to ±30, and the sampling period is 0.002s.

4.1.2 Speed Control Effect

The control effect of brushless DC motor based on STM32 microcontroller increases the load torque from 0 to 5N-m at 0.5s of operation, at which time the change of phase current of the brushless DC motor before and after using the control effect is shown in Fig. 4. As can be seen from the figure, before using the control strategy designed in this paper, the phase current of the brushless DC motor of the agricultural irrigation pump system is in a square wave state, and the fluctuation range is between 7.21A~14.92A before 0.5s, while after increasing the load at 0.5s, its phase current fluctuation range changes to 7.21A~22.84A. At this time, when the brushless DC motor changes phase, the phase current is prone to the problem of sudden changes, which It may lead to changes in the electromagnetic field inside the motor, thus generating additional losses. This kind of loss will not only reduce the efficiency of the motor, but also may cause the motor to heat up, which further affects the performance and reliability of the motor, and it is very easy to have the problem of phase change torque pulsation, and the motor operating efficiency is also negatively affected, which is not conducive to the scientific water saving of the agricultural irrigation pumping system. After adopting the brushless DC motor control strategy

based on STM32 microcontroller in this paper, the phase current is sinusoidal, and the phase current fluctuates in the range of 12.01A~17.75A before or after the load is applied, and the phase current does not show any obvious sudden change. This shows that the intelligent control strategy of the brushless DC motor set in this paper can automatically regulate and smooth the current change during the phase change process, reduce the torque pulsation, make the motor bus current be reasonably controlled, and make the motor phase current smoother, which can provide help for the effective control of the agricultural irrigation pump system.

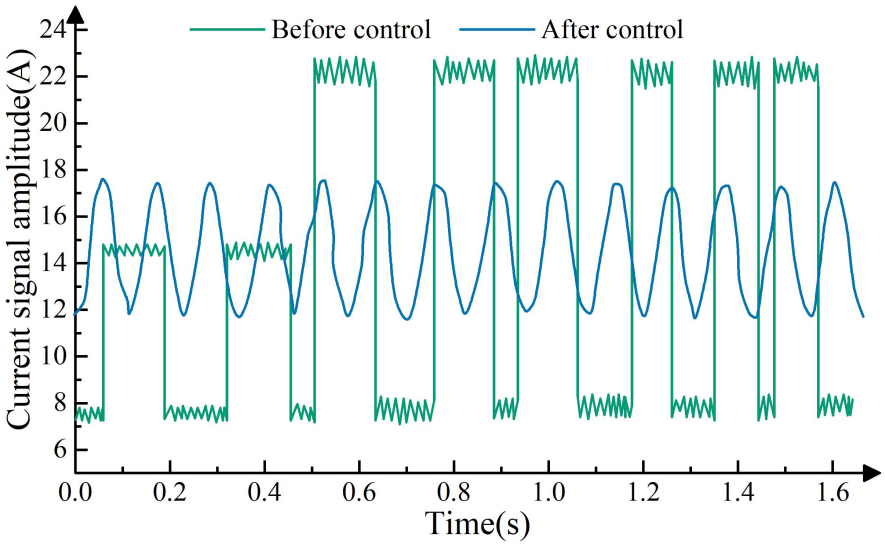

Figure 4 Non-brush direct - type machine phase current change

With the rated speed of 800 r/min, the load torque is increased from 0 to 5 N-m during 0.5 s of operation, and the control effect of the control strategy on the speed of the brushless DC motor is obtained as shown in Fig. 5, where Figs. 5(a)~(b) show the control effect of speed and torque control before and after the implementation of the control strategy, respectively. As can be seen from the figure, the use of STM32 microcontroller-based brushless DC motor control strategy significantly improves the immunity to sudden load changes of the brushless DC motor. When there is a sudden load, the control strategy designed in this paper can quickly and automatically adjust the motor speed to match the desired speed, and the torque does not have abnormal fluctuations, but only weak and smooth changes. In the case of sudden load increase, it shows more significant anti-interference ability and can realize the automatic control of brushless DC motor. This performance is mainly due to the use of STM32

microcontroller in the control strategy, which can automatically adjust the motor speed in the case of sudden load changes. Therefore, the brushless DC motor in the agricultural irrigation pump system in this paper can realize the precise control of irrigation valves and provide effective technical support for agricultural irrigation water saving.

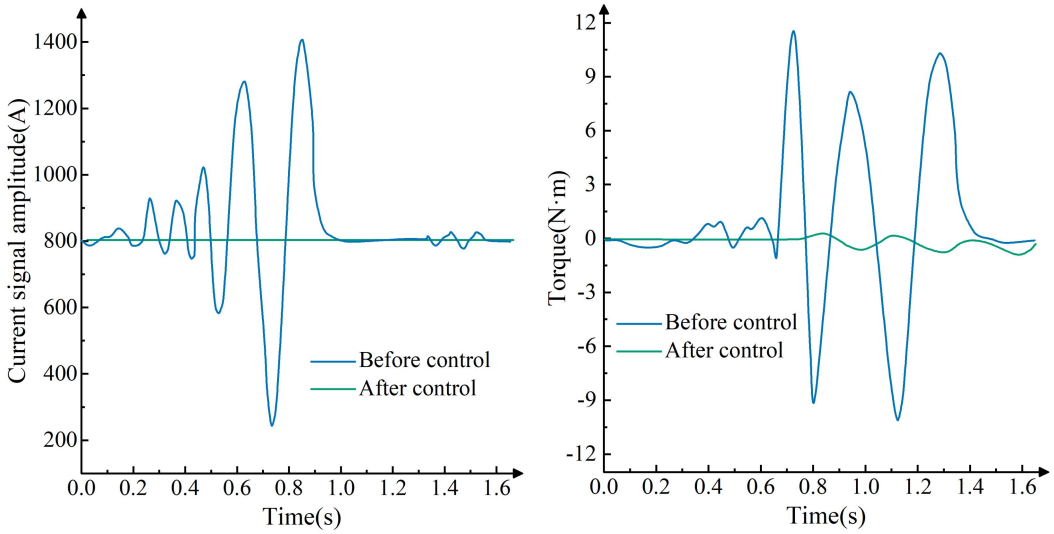

(a) Speed control effect (b) Torque control effect

Figure 5 Speed and torque control effect

4.1.3 Steady-state speed control

In the working process of the agricultural irrigation system, the role of the brushless DC motor is to control the stable operation of the irrigation pump, and in order to verify the feasibility of the control strategy of the brushless DC motor designed in this paper under the steady state speed, in the speed of 4000r/min within the voltage linear modulation zone, from the I/f current amplitude control switched to the PID control, the regulation time of about 0.2s, before and after the PID control of the phase voltage, the phase current The waveforms are shown in Figure 6. Among them, Fig. 6(a)~(b) shows the voltage and current waveforms without adding PID control and PID control, respectively.

After adding PID control at steady state speed, the phase voltage amplitude is reduced from 30.27V to 20.15V, the phase current amplitude is reduced from 1.34A to 0.58A, and the phase difference of phase voltage over phase current is reduced from 45° to 8°. Combined with the space vector diagram of the brushless DC motor, it can

be obtained that after adding PID control, the angle between the motor's reverse electromotive force vector and current vector is reduced to almost zero, and the reactive component of the current and the amplitude of the phase current are reduced.The PID control can effectively reduce the rms and peak values of the current, so as to make the motor run in the state of the maximum torque/current ratio, and to improve the efficiency of the brushless DC motor. And the efficiency improvement of brushless DC motor in agricultural irrigation system can significantly enhance the control efficiency of irrigation pumps and provide support for efficient irrigation and scientific water saving.

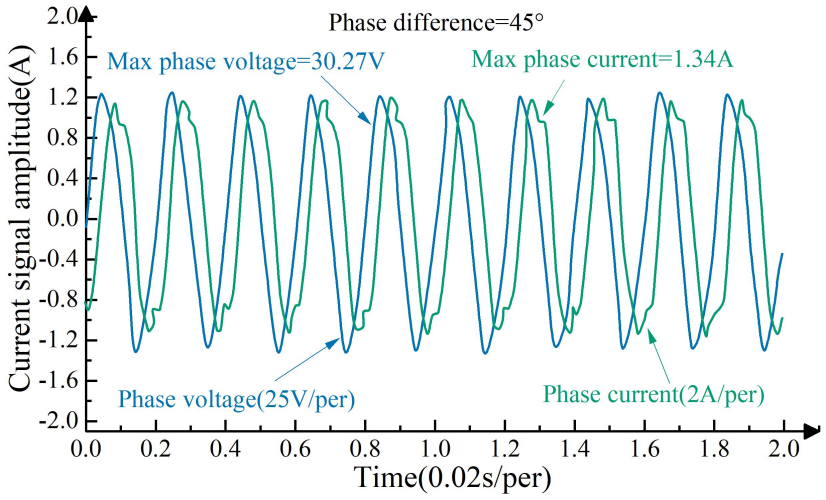

(a) Before PID control

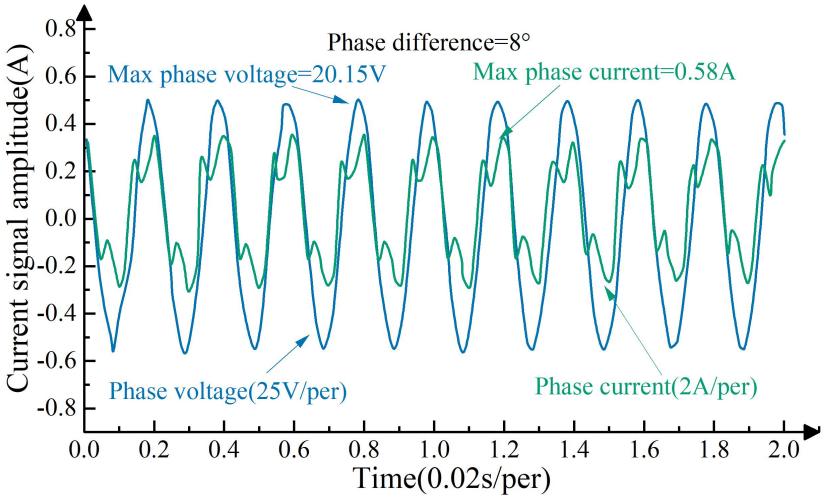

(b) After PID control

Figure 6 Voltage and current waveforms before and after PID control

4.2 Measurement of the effective utilization factor of irrigation water

4.2.1 Net Irrigation Water in Irrigation Districts

The research object selected for this paper is the Shule River Basin, which is located in the westernmost part of the Hexi Corridor in Province G. The average annual runoff is more than 1,018 million m^3, the average annual precipitation is less than 40-50 mm, and the annual evaporation reaches more than 2,400 mm, which is one of the extremely arid regions in China. 3 reservoirs, CM, ST and CJX, have a total capacity of 471.9 million m^3, and the length of main channels is $2.85*10^4$ km. 104km, 82 branch canals, 624 bucket canals and 6306 agricultural canals. There are three irrigation districts, CM, ST and CJX, in the Shule River Basin, with an irrigated area of 1,343,600 mu. The three major irrigation districts have now been designated as model irrigation districts for effective utilization of agricultural irrigation water in Province G.

Taking the CM and ST sample point irrigation districts as the research object, based on their data in 2022, the net irrigation water volume calculation method given in the previous section is used to calculate the net irrigation water volume of typical fields in each irrigation district. Then, using the agricultural irrigation system designed in this paper, the simulation value of the net irrigation water volume of typical fields was calculated through simulation, and the net irrigation water volume of typical fields in the sample point irrigation areas was obtained as shown in Table 1.

From the table, it can be seen that the combined net irrigation water volume of pepper, sand nut and citrus in the irrigation area of CM sample site in 2022 is 3724.51, 3059.48 and 2342.95m^3/hm^2, while the combined net irrigation water volume of potato is 0m^3/hm^2. After using the agricultural irrigation pump system designed in this paper for scientific water conservation control, the simulated integrated net irrigation water quantities of pepper, sand nut and citrus in the irrigation area of the CM sample site were 2539.24, 2351.82 and 1816.46m^3/hm^2, respectively, which were reduced by 31.82%, 23.13% and 22.47%, respectively, compared with the actual integrated net irrigation water quantities. In addition, the integrated net irrigation water volume of

pepper and roasted tobacco in the irrigation area of the ST sample site was 3208.24 and 493.63 m^3/hm^2, respectively, and the integrated net irrigation water volume of pepper and roasted tobacco after utilizing the agricultural irrigation pumping system was 1726.38 and 281.75 m^3/hm^2, which was lower than that of the actual net irrigation water volume by 1481.86 and 211.88 m^3/hm^2, respectively. Under the condition of ensuring the actual irrigated area remains unchanged, the agricultural irrigation pump system designed in this paper can significantly reduce the net irrigation water volume and achieve effective irrigation water saving, which can effectively meet the needs of crop irrigation water volume and realize high water saving benefits.

Table 1 Typical farmland net irrigation water quantity

Sample area	Crop name	Net irrigation water (m^3/hm^2)		Actual area of irrigation (hm^2)		Total net irrigation water ($*10^4m^3$)	
		Actual	Analog	Actual	Analog	Actual	Analog
CM	Prickly ash	3724.51	2539.24	1321.38	1321.38	495.46	281.75
	Sand kernel	3059.48	2351.82	305.57	305.57	94.38	70.12
	Citrus	2342.95	1816.46	372.06	372.06	83.73	66.59
	Potato	0.00	0.00	157.43	157.43	0.00	0.00
ST	Prickly ash	3208.24	1726.38	231.39	231.39	74.21	37.94
	Cured smoke	493.63	281.75	80.06	80.06	3.98	1.76

4.2.2 Effective utilization factor of irrigation water

Since the three major irrigation districts of CM, ST and CJX have been identified as the provincial typical sample irrigation districts, the management units of the irrigation districts have earnestly followed the requirements of the work, and have continuously strengthened the analysis and measurement of the utilization rate of the canal system at all levels, and have strictly measured the efficiency of the utilization of the irrigation water from the hopper to the field. Based on the data from 2010 to 2021 of the three major irrigation districts of CM, ST and CJX, combined with the comprehensive net irrigation water volume in 2022 obtained by simulation in the previous subsection, and then based on the calculation method of effective utilization coefficient of irrigation water given in the previous section, the effective utilization coefficients of irrigation water in the three major irrigation districts for the period of 2010 to 2022 are obtained as shown in Fig. 7.

The analysis and study of the effective utilization coefficient of irrigation water in the three major irrigation districts from 2010 to 2022 showed that the effective utilization coefficient of irrigation water increased year by year. This may be related to the increase in the area of canal lining and efficient water-saving irrigation, and the increase was significantly higher from 2012.In 2015, compared with 2010, the effective utilization coefficient of irrigation water in CM irrigation district, ST irrigation district, and CJX irrigation district increased by 0.053, 0.03, and 0.044, respectively, and the increase in the effective utilization coefficient of irrigation water in the three major irrigation districts reached 10.93%, 10.93%, 10.93%, 6.65%, and 9.44%, 6.65% and 9.32% respectively. It shows that since 2010, with the increasing investment in the construction and renovation of the three irrigation districts, through the project approval and implementation of the Comprehensive Plan for Rational Utilization of Water Resources and Ecological Protection, the irrigation districts have constructed a series of irrigation follow-up projects and water-saving and renovation projects, the channel projects have been continuously improved, and the completion rate of the irrigation districts' water distribution and allocation projects has been significantly increased, which greatly reduces the losses of the channels in terms of transmission and distribution and seepage. The improvement of irrigation district management level has also led to an effective increase in the utilization rate of water resources. In addition, the effective utilization coefficient of irrigation water in the three major irrigation districts before 2021 did not exceed 0.6, while in the simulation results of the agricultural irrigation pump system designed in this paper with the support of brushless DC motor, the effective utilization coefficients of the irrigation water in the three major irrigation districts reached 0.614, 0.602, 0.616, which to some extent explains the effectiveness of the agricultural irrigation pump system designed in this paper in rational planning and application of irrigation water, and can significantly improve the irrigation water utilization rate. The effectiveness of the application can significantly improve the effective utilization rate of irrigation water and provide a new technical example for the realization of scientific water conservation.

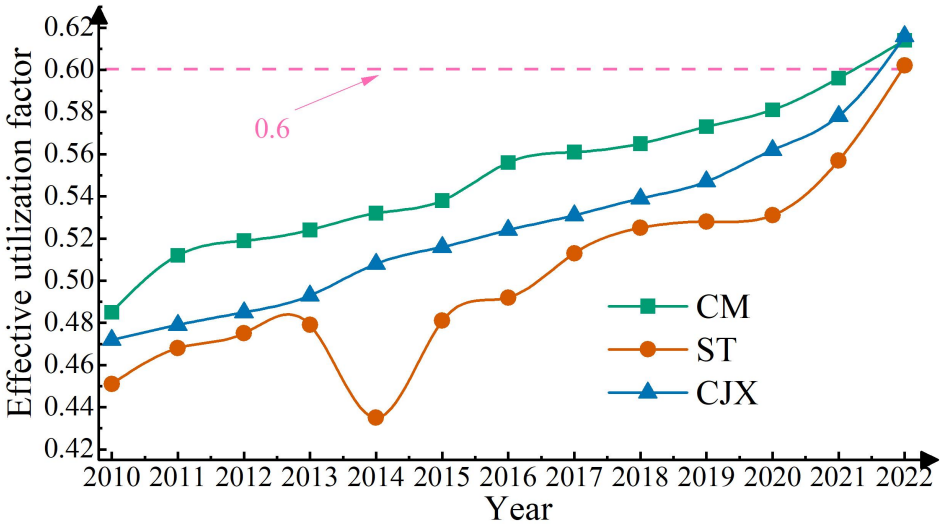

Figure 7 The effective utilization coefficient of irrigation water in 2010~2022

4.3 Validation of the effectiveness of the irrigation pumping system

4.3.1 Accuracy testing of irrigation

Taking pepper crops in the CT sample irrigation area as an example, two groups of replicated tests were set up to verify the irrigation accuracy of the system for 15 days. According to the existing research, it is known that under indirect subsurface drip irrigation of dwarfed and densely planted peppers, the soil layer with the largest water content appeared in the range of 16~32cm, therefore, the soil moisture sensors were set up to be buried at a depth of 12cm, 26cm, and 35cm from the ground surface, and the soil temperature sensors at a depth of 12cm and 26cm, and a horizontal distance of 8cm from the trunk of the tree. In the case of the highest water utilization, the soil moisture content varies from 7.5% to 14.5% (as a percentage of dry soil weight) in the 12~42cm soil layer. Since the value measured by the soil moisture sensor is the relative soil moisture content, if the relative soil moisture content is to be obtained, it can be derived from the volumetric soil moisture content. Pepper soil surface texture is sandy loam, soil density 1.41g/cm³, field water holding capacity is 29.15%, which is converted to the soil relative water content between 33.5% and 70.8%, and set this threshold for autonomous irrigation. The results of the irrigation test using the agricultural irrigation pump system constructed in this paper in combination with a brushless DC motor are shown in Table 2.

It can be seen from the data in the table that the agricultural irrigation pump system designed in this paper can automatically irrigate according to the set irrigation threshold and report the irrigation completion information and alarm information in real time, and the manual control can be effectively realized and will not conflict with the automatic irrigation. When the relative soil moisture content is lower than 33.5% of the lower limit of the system alarm at the same time will automatically irrigate, when higher than 70.8% of the system will stop irrigation, indicating that the system can be set according to the moisture content of stable irrigation. It can ensure the effective irrigation of crops and at the same time, better save water resources and realize the rationalization of agricultural irrigation water application.

Table 2 Irrigation test for agricultural irrigation pump system

Test type	This system			Manual irrigation
Date	2023.08.10	2023.08.16	2023.08.22	2023.08.23
Threshold setting	33.5%~70.8%			-
Soil water rate irrigation trigger value	≤32.5%~33.5%	≤33.5%	≤32.5%~33.5%	-
Soil moisture content irrigation stop value	≥70.8%~71.2%	≥70.8%~71.2%	≥70.8%	-
Whether Irrigation completion	YES	YES	YES	YES
Whether to send a manual irrigation instruction	NO	NO	NO	YES
Whether alarm	NO	NO	NO	NO

4.3.2 Irrigation flow error testing

Prior to the actual application of the hardware irrigation module of the agricultural irrigation pumping system, the Hall flow sensor needs to be commissioned to determine the actual accuracy of the device in order to determine the actual error of the irrigation. Flow sensor installed in the peristaltic pump rear position used to detect the water flow. Flow sensor pipe diameter of 6.8mm, with a measuring cylinder for each single pipeline for the total amount of irrigation readings, with a stopwatch to record the time of each irrigation, the experiment was repeated 10 times, the experiment was set to irrigate each time the amount of 50ml, the calculation of the

hardware of the irrigation error. The statistical results of the flow sensor error of the agricultural irrigation pump system are shown in Table 3. As can be seen from the table, the average irrigation time is 29.99s, and the average error of irrigation water flow is only 0.994%, which is in line with the irrigation accuracy requirements of this design in terms of the irrigation accuracy of the hardware.

Table 3 Flow sensor error statistics

Load voltage (V)	Irrigation time (s)	Actual flow (mL)	Flow sensor value (mL)	Error (%)
12.03	31.54	40.39	40.23	0.40
11.97	30.73	40.18	39.95	0.57
11.95	29.38	39.42	39.24	0.46
12.02	29.95	38.95	38.51	1.13
12.13	30.74	38.47	38.06	1.06
11.69	28.86	39.83	39.17	1.66
12.07	31.24	40.35	39.92	1.07
11.89	28.01	40.42	39.78	1.58
12.06	30.13	41.29	40.85	1.07
12.04	29.32	41.43	41.04	0.94

In order to ensure the applicability of the system in the regional experiment, the irrigation experiment selected the values of crop coefficient K_c in different cycles of the growth of tobacco varieties planted in the irrigation area of the ST sample site as the calculation factor for calculating the crop water demand, in which the seedling and three-leaf period of tobacco is the early growth period, the period K_c value is 0.12, the bud stage and the flower bell stage is the mid-growth period, the period K_c value of 1.13~1.22, and the late-growth stage of the K_c value of 0.65~0.85. 0.65~0.85, in this experiment, the crop coefficient of 1.22 at the middle stage of growth of roasted tobacco was selected as the coefficient required for experimental calculation. The experimental period was from July 22, 2022 to August 18, 2022, and the day-by-day meteorological data of the ST area during this time period were used as inputs, including the five elements of maximum temperature, minimum temperature, relative humidity, average wind speed, and sunshine duration, and the data were obtained from the China Meteorological Data Network (CMDN).

The above meteorological factor data imported into the crop transpiration model established in the previous section, the corresponding site within the software of the agricultural irrigation pumping system in order to call the prediction model, the crop species selection of roasted tobacco option box, the growth stage selection of mid-fertility crop coefficients are automatically adjusted to 1.22, 20 prediction experiments were carried out, resulting in the results of the test as shown in Figure 8. In the figure, ET is the crop water demand, and ET0 is the crop transpiration.

From the data distribution in the figure, it can be seen that the error between the predicted irrigation amount and the actual irrigation amount of the agricultural irrigation pump system combined with the brushless DC motor is no more than 3.57%, and the average error of the irrigation of crop water demand is only 1.02%. This shows that the agricultural irrigation pump system constructed by combining brushless DC motor in this paper can realize accurate prediction of crop water demand and quantitative irrigation, which can provide reliable technical support for rational water use in agricultural irrigation and maximize the application of water resources in agricultural irrigation.

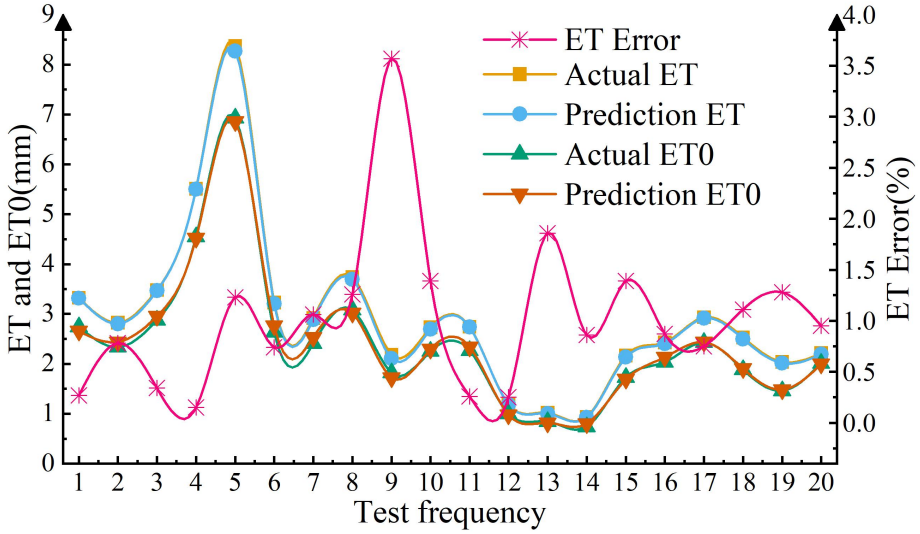

Figure 8 System platform overall testing

5. Conclusion

The article proposes an STM32-based brushless DC motor control system for agricultural irrigation pumps, and carries out a validation analysis for the application effectiveness of the system. After adopting the control strategy based on STM32

microcontroller, the phase current of the brushless DC motor of the agricultural irrigation pump system was sinusoidal, and its phase current fluctuation range was stabilized in the range of 12.01A~17.75A without any obvious sudden change. After the introduction of the agricultural irrigation pump system in the ST sample irrigation area, the integrated net irrigation water volume of pepper and tobacco was 1726.38 and 281.75 m^3/hm^2, respectively, which was lower than the actual net irrigation water volume by 1481.86 and 211.88 m^3/hm^2, respectively. And the maximum error between the predicted irrigation amount and the actual irrigation amount of the agricultural irrigation pumping system does not exceed 3.57%, and the average error of the irrigation of crop water demand is only 1.02%. Relying on the brushless DC motor controlled by STM32, it can make the agricultural irrigation pump system realize the fine irrigation water control, and provide a guarantee to promote the scientific use of agricultural irrigation water.

References

[1] Wang, Z., Li, J., & Li, Y. (2017). Using reclaimed water for agricultural and landscape irrigation in China: a review. Irrigation and drainage, 66(5), 672-686.

[2] Wang, J., Zhu, Y., Sun, T., Huang, J., Zhang, L., Guan, B., & Huang, Q. (2020). Forty years of irrigation development and reform in China. Australian Journal of Agricultural and Resource Economics, 64(1), 126-149.

[3] Xu, L., Shi, Z., Wang, Y., Chu, X., Yu, P., Xiong, W., ... & Zhang, S. (2017). Agricultural irrigation-induced climatic effects: a case study in the middle and southern Loess Plateau area, China. International Journal of Climatology, 37(5), 2620-2632.

[4] Wang, J., Zhang, Z., & Liu, Y. (2018). Spatial shifts in grain production increases in China and implications for food security. Land use policy, 74, 204-213.

[5] Ma, W., Liu, T., Li, W., & Yang, H. (2023). The role of agricultural machinery in improving green grain productivity in China: Towards trans-regional operation and low-carbon practices. Heliyon, 9(10).

[6] Askaraliev, B., Musabaeva, K., Koshmatov, B., Omurzakov, K., &

Dzhakshylykova, Z. (2024). Development of modern irrigation systems for improving efficiency, reducing water consumption and increasing yields. Machinery & Energetics, 15(3).

[7] Lakhiar, I. A., Yan, H., Zhang, C., Wang, G., He, B., Hao, B., ... & Rakibuzzaman, M. (2024). A review of precision irrigation water-saving technology under changing climate for enhancing water use efficiency, crop yield, and environmental footprints. Agriculture, 14(7), 1141.

[8] Xudayev, I. J., Fazliev, J. S., & Ayusupova, A. (2021, October). Water saving up-to-date irrigation technologies. In IOP Conference Series: Earth and Environmental Science (Vol. 868, No. 1, p. 012040). IOP Publishing.

[9] Juraev, F., & Karimov, G. (2020, July). Water saving technique and technology of subsurface irrigation. In IOP Conference Series: Materials Science and Engineering (Vol. 883, No. 1, p. 012095). IOP Publishing.

[10] Ashari, M., Rivai, M., & Mustaghfirin, M. A. (2018, August). Energy consumption of brushless dc motor for modern irrigation system. In 2018 International Seminar on Intelligent Technology and Its Applications (ISITIA) (pp. 105-110). IEEE.

[11] Suwito, S., Ashari, M., Rivai, M., & Mustaghfirin, M. (2018, October). Implementation of water pressure control on drip irrigation systems using a centrifugal water pump driven by a brushless DC motor. In AIP Conference Proceedings (Vol. 2021, No. 1). AIP Publishing.

[12] Kumar, R., & Singh, B. (2017). Single stage solar PV fed brushless DC motor driven water pump. IEEE Journal of Emerging and Selected Topics in Power Electronics, 5(3), 1377-1385.

[13] Singh, B., & Kumar, R. (2016). Simple brushless DC motor drive for solar photovoltaic array fed water pumping system. IET Power Electronics, 9(7), 1487-1495.

[14] Hasan, M., Alhazmi, W. H., & Zakri, W. (2022). A fuzzy rule based control algorithm for MPPT to drive the brushless dc motor based water pump. Journal of Intelligent & Fuzzy Systems, 42(2), 1003-1014.

[15] Nisha, R., & Sheela, K. G. (2020). Review of PV fed water pumping systems using BLDC Motor. Materials Today: Proceedings, 24, 1874-1881.

[16] Singh, B., & Kumar, R. (2016). Solar photovoltaic array fed water pump driven by brushless DC motor using Landsman converter. IET Renewable Power Generation, 10(4), 474-484.

[17] Shukla, T., & Nikolovski, S. (2023). A solar photovoltaic array and grid source-fed brushless dc motor drive for water-pumping applications. Energies, 16(17), 6133.

[18] Kumar, R., & Singh, B. (2018). Brushless DC motor-driven grid-interfaced solar water pumping system. IET Power Electronics, 11(12), 1875-1885.

[19] Dheepika, R., Nishanth, G., & Ahamed, S. (2024). Solar Powered Water Pump with Zeta Converter and BLDC Motor. Educational Administration: Theory and Practice, 30(6), 1919-1927.

[20] Kumar, A., Marwaha, S., Manna, M. S., Marwaha, A., Kumar, R., Amir, M., ... & Zaitsev, I. (2025). Comparative analysis of brushless DC and switched reluctance motors for optimizing off-grid water pumping. Scientific Reports, 15(1), 3527.

[21] Lais, A., Abhijith, R. S., Akash, M. R., Danish, J., & Varghese, B. M. (2019). IoT Enabled BLDC motor Driven Water Pump Employing Zeta Converter. International Research Journal of Engineering and Technology, 6(6), 2593-2599.

[22] Sevugan Rajesh, J., Karthikeyan, R., & Revathi, R. (2024). Analysis and control of grid-interactive PV-fed BLDC water pumping system with optimized MPPT for DC-DC converter. Scientific Reports, 14(1), 25963.

[23] Kumar, R., & Singh, B. (2019). Grid interactive solar PV-based water pumping using BLDC motor drive. IEEE Transactions on Industry Applications, 55(5), 5153-5165.

[24] Antony, R. P., Komarasamy, P. R. G., Rajamanickam, N., Alroobaea, R., & Aboelmagd, Y. (2024). Optimal Rotor Design and Analysis of Energy-Efficient Brushless DC Motor-Driven Centrifugal Monoset Pump for Agriculture Applications. Energies, 17(10), 2280.

[25] Gautam, S. K., & Kumar, R. (2023). Synchronisation of solar

PV-wind-battery-based water pumping system using brushless DC motor drive. International Journal of Power Electronics, 18(4), 435-459.

[26] Henning Bjornlund,Karen Parry,Andre van Rooyen & Jamie Pittock. (2025). Critical reflections on transforming smallholder irrigation systems from dysfunctional to functional climate smart agricultural systems. International Journal of Water Resources Development(2),223-228.

[27] Tripathi Amita,Tiwari Pankaj Kumar,Misra Arvind Kumar & Kang Yun. (2022). Impacts of transpiration of agricultural crops and seeding on rainfall: Implications from a mathematical model. International Journal of Biomathematics(05).

[28] Wei Shi,Wengang Zheng,Feng Feng,Xuzhang Xue & Liping Chen. (2025). Influence of Combinations of Estimated Meteorological Parameters on Reference Evapotranspiration and Wheat Irrigation Rate Calculation, Wheat Yield, and Irrigation Water Use Efficiency. Water(2),138-138.

[29] K Fathoni,E Apriaskar,N A Salim,S Hidayat,A F Suni,A F Hastawan & N Iksan. (2024). Performance Investigation of Model Predictive Control for Brushless DC Motor. IOP Conference Series: Earth and Environmental Science(1),012009-012009.

[30] Pan Zhang,Zhaoyao Shi,Bo Yu & Haijiang Qi. (2024). Research on the Control Method of a Brushless DC Motor Based on Second-Order Active Disturbance Rejection Control. Machines(4).